Properties of local plasma injections in Saturn's magnetosphere

J. L. Burch,[1] J. Goldstein,[1] T. W. Hill,[2] D. T. Young,[1] F. J. Crary,[1] A. J. Coates,[3] N. André,[4] W. S. Kurth,[5] and E. C. Sittler Jr.[6]

Received 2 February 2005; revised 12 March 2005; accepted 25 March 2005; published 1 June 2005.

[1] Electron and ion drift dispersion events are often observed by the Cassini Plasma Spectrometer (CAPS) in the inner magnetosphere of Saturn (5 to 10 R_S). These events appear to result from azimuthally-limited injections of plasma and persist for at least several hours. During this time, the events can be analyzed to obtain information on the time and azimuthal location of the injections. The CAPS data show evidence of both remote and local injections. In this paper a conceptual model of Saturnian centrifugal interchange is developed based on the characteristics of the local injections. **Citation:** Burch, J. L., J. Goldstein, T. W. Hill, D. T. Young, F. J. Crary, A. J. Coates, N. André, W. S. Kurth, and E. C. Sittler Jr. (2005), Properties of local plasma injections in Saturn's magnetosphere, *Geophys. Res. Lett.*, *32*, L14S02, doi:10.1029/2005GL022611.

1. Introduction

[2] Transport in the interior of a rapidly rotating magnetosphere is expected to be dominated by internally-driven convection [*Hill et al.*, 1981] rather than by solar-wind-driven convection, with centrifugal interchange [*Hill*, 1976; *Siscoe and Summers*, 1981] possibly also playing an important role. These expectations were borne out by the Galileo measurements at Jupiter's Io torus [e.g., *Thorne et al.*, 1997; *Kivelson et al.*, 1997]. The Cassini data [*Mauk et al.*, 2005; *Hill et al.*, 2005] show that Saturn's inner magnetosphere is clearly rotation-dominated and provide evidence of widespread occurrence of azimuthally-limited plasma injections. The signatures of these injections include drift dispersion events, in which electrons and ions of various energies are separated azimuthally with time, with the separations becoming more pronounced at large azimuthal separations between the injection and the spacecraft (i. e., for remote injections).

[3] The Cassini Plasma Spectrometer (CAPS) [*Young et al.*, 2004] observed both remote and local injections during the period of the Saturn orbit injection on June 30 and July 1, 2004. Evidence that centrifugal interchange is responsible for the local injections includes the deep density gradients and the heated plasma distributions that are observed within them. The drift dispersion events that develop over periods of hours following the injections contain information on the local time, extent, and energy spectra of the injected electrons and ions. *Hill et al.* [2005] have mapped the locations of numerous such remote injections based on the characteristics of the drift dispersion events, and *Mauk et al.* [2005] demonstrate the expected effects of subcorotation [*Richardson and Sittler*, 1990] on them.

[4] The characteristics of the local injections are consistent with expectations for centrifugal interchange events in which distant magnetic flux tubes containing hot, tenuous plasmas convect inward to replace flux tubes containing dense, cold plasma. Within the density cavities, drift dispersions, similar to those observed in the remote injections, occur in the high-energy part of the electron and ion distributions but with the decreasing ion energies and increasing electron energies observed simultaneously instead of sequentially as is the case with the remote injections.

[5] A model is presented that produces the major features of the remote and local injections. In this model, drift dispersion occurs within an interchanging flux tube while it convects inward through the inner Saturnian magnetosphere. When the interchange event crosses the planetary radial distance of Cassini near the spacecraft it rotates over it at or near the corotation speed, producing the dispersion signatures of falling ion energies and rising electron energies. After injection, the drifting electrons and ions eventually leave the density cavity by magnetic drifts and are observed to display the characteristics of remote injections (falling ion energies followed by rising electron energies).

2. Observations

[6] The data used in this study were obtained by CAPS on July 1, 2004 when the spacecraft was outbound approximately 10° south of the equatorial plane. CAPS consists of an electron spectrometer (ELS), an ion mass spectrometer (IMS) and an ion beam spectrometer (IBS) mounted on a rotating platform. In this analysis, data from the ELS and the IMS (total ion measurements only) are used. During this time period the rotating platform was held at a fixed position yielding partial 2-D angular distributions.

[7] Figure 1 shows an energy-time spectrogram of ELS and IMS data along with line plots of total electron density from ELS (1 eV to 28 keV), the low-energy limit of significant fluxes in IMS (superimposed on the spectrogram and plotted again in the bottom panel), and $10/n_e$. The ELS densities (n_e), which are roughly consistent with measurements of the upper hybrid wave frequency by the Cassini plasma wave instrument [*Gurnett et al.*, 2004], assume an isotropic distribution, so they should be considered as upper limits. The excellent correlation between ion energy lower

[1]Southwest Research Institute, San Antonio, Texas, USA.
[2]Rice University, Department of Physics and Astronomy, Houston, Texas, USA.
[3]Mullard Space Science Lab, University College London, Dorking, Surrey, U. K.
[4]Centre d'Etude Spatiale des Rayonnements, Toulouse, France.
[5]University of Iowa, Department of Physics and Astronomy, Iowa City, Iowa, USA.
[6]NASA, Goddard Space Flight Center, Greenbelt, Maryland, USA.

0094-8276/05/2005GL022611

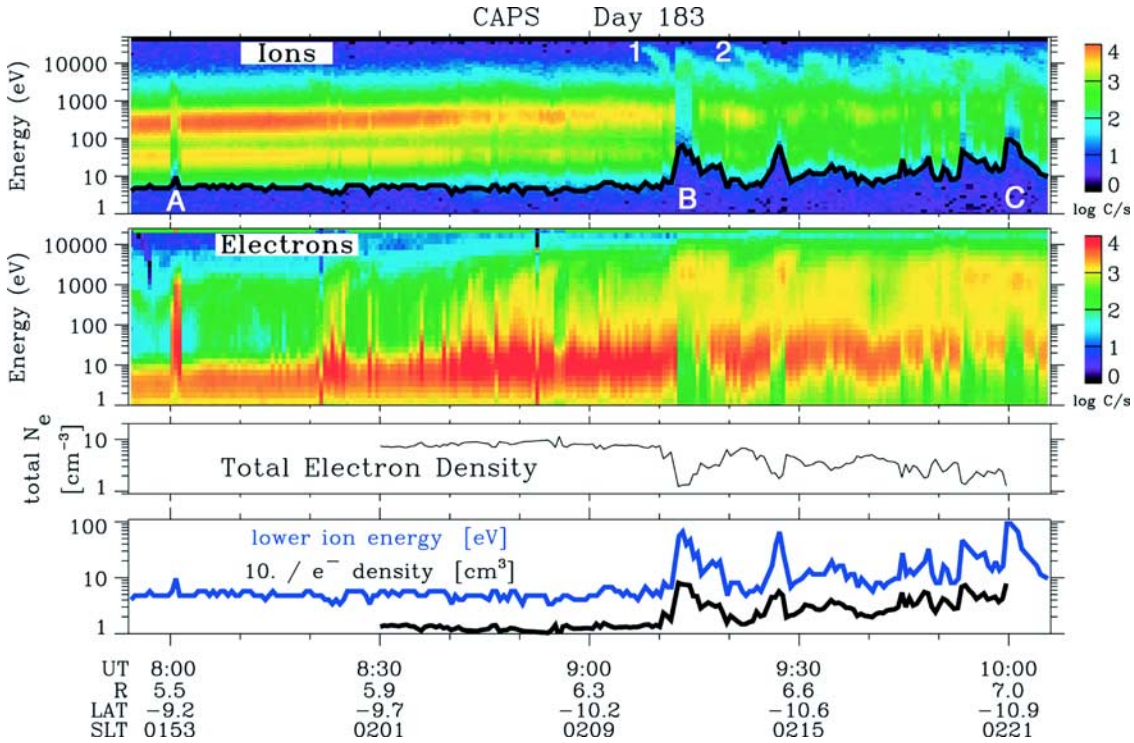

Figure 1. Energy-time count-rate spectrograms of total ions and electrons at pitch angles near 80°. Superimposed on the ion spectrogram is a trace of the lowest ion energy with significant counts. Also shown are electron density computed from the ELS data (third panel) and a repeat of the ion low-energy threshold plot and the inverse of the electron density multiplied by ten (bottom panel).

limit and $10/n_e$, shown in the bottom panel, provides evidence that flux tubes containing plasmas with lower densities and higher temperatures are replacing colder, more dense plasmas, as is expected from centrifugal interchange. Noted in the IMS spectrogram are two examples of remote plasma injections (1 and 2) and three examples of local plasma injections (A, B, and C).

[8] The remote injections (1 and 2) in Figure 1 have the shape of drift dispersion events as illustrated in the computed example in Figure 2, which shows energy-time traces of equatorially-mirroring ions and electrons that would result from an injection 7.56 R_S to the west of an observation point at R = 6.5 R_S in the dipole-approximated magnetic field. Energy-flux ion spectra for remote injection event 1 are shown in Figure 3a. The sequentially-observed spectra show relatively narrow energy peaks that move linearly toward lower energies with time. These features are consistent with the predictions of magnetic drift dispersion.

[9] The dispersions within the local injections have similar energy-time slopes to those of the remote injections but with the important differences that (1) the ion and electron dispersions are observed together and (2) the dispersions appear as progressions of high-energy cutoffs rather than of energy-flux peaks. Ion energy-flux spectra for local injection event B are shown at five successive times in Figure 3b. The high-energy tails of the energy-flux spectra in Figure 3b progress toward lower energies at a rate that is approximately linear with time as was the case with the remote injections. Thus it can be concluded that these

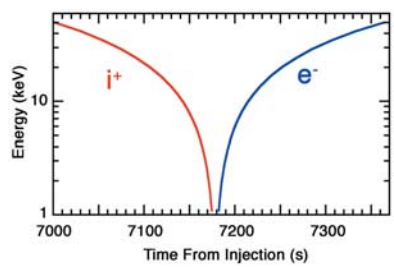

Figure 2. Computed drift dispersion curves for electrons and ions injected at R = 6.5 R_S at a local time 7.56 R_S to the west of an observation point in the dipole-approximated Saturn magnetic field.

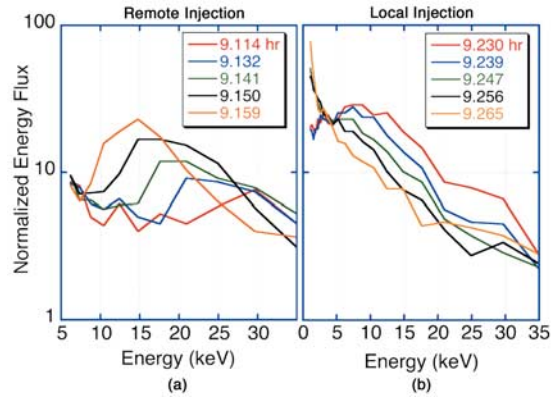

Figure 3. (a) Ion energy-flux spectra for the remote injection event 1 in Figure 1. (b) Ion energy-flux spectra for the local injection event B in Figure 1.

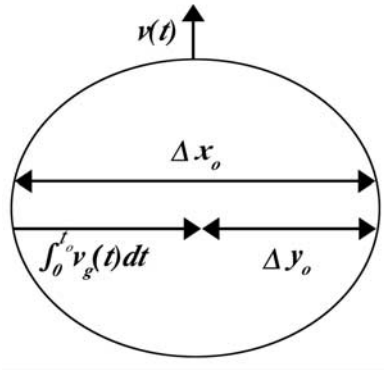

Figure 4. Sketch of an equatorial cut of an interchange flux tube showing its planetward velocity, $v(t)$, its width at the observation point, Δx_o, the total gradient drift distance at time t_o, $\int_0^{t_o} v_g(t)dt$, and the remaining distance to the boundary of the flux tube, Δy_o.

spectra, although different in character from those of the remote injections, might also result from magnetic drift dispersion.

3. Conceptual Model

[10] The sharp boundaries of the density cavities and the fact that the energy dispersions are wholly contained within them suggest the existence of isolated magnetic flux tubes containing hot, low-density plasma convecting planetward into a colder, higher-density region, as would result from centrifugal interchange. A simple test of this idea can be made using the conceptual model in Figure 4. At $t = 0$, a dipole flux tube at $R = R_1$ is uniformly filled with ions and electrons. As time progresses, the flux tube moves radially inward (in the rotating frame) at a velocity $v(t)$, and its width decreases. During this motion, the equatorially-mirroring ions and electrons undergo gradient drift (v_g) in the rotating frame. Eventually, the highest energy particles will drift completely out of the convecting flux tube and will be trapped in the surrounding magnetic field. At a time t_o, only a fraction of the flux tube (given by $\Delta y_o/\Delta x_o$) will contain particles above a given energy $W_{\perp o}$. In the rotating frame, the ions will drift toward the eastern edge of the flux tube, while the electrons will drift toward its western edge. The distance Δy_o (Figure 4) at a radius R_o is,

$$\Delta y_o = \Delta x_o - \int_0^{t_o} \frac{\Delta x_o v_g(t)}{\Delta x(t)} dt \tag{1}$$

where the ratio $\Delta x_o/\Delta x(t)$ scales the drift to the changing cavity width. Assuming that the interchanging flux tubes maintain their dipole topology throughout the process, $\Delta x(t) = \Delta x_o[R(t)/R_o]$ and $v_g(t) = 3W_\perp/qBR(t)$. Conservation of the first adiabatic invariant leads to $W_\perp/B$ being a constant. Then the fraction of the interchanging flux tube that would contain particles with energy $W_{\perp o}$ at $t = t_o$ (the rest having drifted out of the flux tube) is given by,

$$\frac{\Delta y_o}{\Delta x_o} = 1 - \frac{3W_{\perp o}R_o}{q\Delta x_o B_o} \int_0^{t_o} \frac{dt}{[R(t)]^2} \tag{2}$$

where $R(t) = R_1 - \int_0^t v(t)dt$, and $v(t)$ is the inward velocity of the interchanging flux tube. Under the assumption of a constant velocity, $R(t) = R_1 - vt$, and the fraction of the flux tube occupied by particles with energy $W_{\perp o}$ is given by,

$$\frac{\Delta y_o}{\Delta x_o} = 1 - \frac{3W_{\perp o}R_o}{q\Delta x_o B_o} \int_0^{t_o} (R_1 - vt)^{-2} dt = 1 - \frac{3W_{\perp o}}{q\Delta x_o B_o v}(1 - R_o/R_1) \tag{3}$$

The free parameters in equation (3) are v and R_1. If one of these parameters could be determined, then the other could be estimated by fits to the CAPS data.

[11] We note that the assumption v = constant is an oversimplification and that, for an interchange instability that develops finger-like intrusions of plasma [*Yang et al.*, 1994], the dipole approximation for the variation of Δx along the interchange path could be invalid. Other, more complex estimates would have to be made, and that is why the model presented here is only conceptual. Thus any comparisons with the Cassini data can only test the general applicability of the simple convection plus gradient drift model. Figure 5 shows such a comparison for local injection event A, which occurred at $R_o = 5.52$ R_S. $R_1 = 10$ R_S and $v =$ 25 km/s, were used to compute the red histogram traces in Figure 5. According to the conceptual model, energies below the red histograms would be allowed, while higher energies would be forbidden within the density cavities.

[12] After the interchange flux tube crosses a particular observation radius the particles that drift out of it will form a remote dispersion event at large distances to the east of the injection. On the other hand, for observation points near the crossing, the local injection signature, with electron and ion

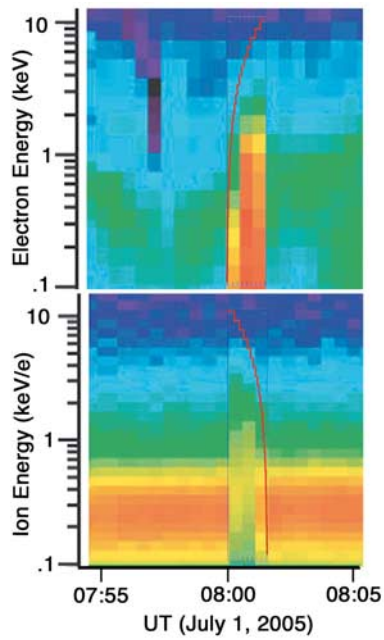

Figure 5. Energy-time spectrograms through local injection event A in Figure 1. Superimposed in red on the spectrograms are the electron and ion dispersion curves calculated from equation (2) for an injection at 10 R_S and a planetward flux-tube interchange velocity of 25 km/s.

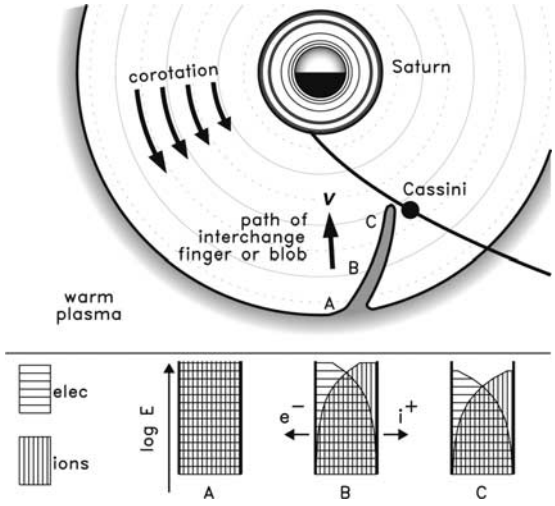

Figure 6. Sketch of an interchange finger (density cavity) in a Saturn-fixed frame of reference. The inward velocity of the finger in the corotating frame is *v*. In the bottom panel, electron and ion dispersions are shown at three distances using equation (3) with R_1 = 12 R_S, v = 50 km/s, and a cavity dimension at 6.5 R_S (point C) of 9000 km.

dispersions observed together totally within the density cavity, will be observed as the flux tube rotates over the observation point.

4. Summary and Conclusions

[13] Figure 6 is a sketch of the described sequence of events. An interchanging flux tube penetrates deep into the magnetosphere along the shaded path, bringing with it a density cavity and hot plasma, both of which are characteristic of the environment at larger distances. For the observation of a local injection, the injection cavity must cross the Cassini distance fairly near the spacecraft in local time (a few minutes of corotation time) and then rotate over it before there is significant leakage of energetic particles out of the density cavity. The bottom part of Figure 6 shows the predicted energy dispersions in the rotating frame as they develop within the cavity at points A, B, and C along its path. At point A, the cavity is uniformly filled with plasma up to the highest energies contained in the ambient population. By point B, the most energetic ions and electrons have drifted out of the cavity and will form remote injection signatures for any observer at a large local-time separation at that radial distance. By point C, the energy dispersions have developed to lower energies. For this sketch, an injection distance of 12 R_S and a flux-tube velocity (radially inward in the rotating frame of reference) of 50 km/s were used with an observation point (C) at 6.5 R_S (where the corotation velocity is 63 km/s) and a density cavity width of 9000 km (roughly nine times the gyroradius of a 20 keV oxygen ion). These parameters produce dispersions such as those observed at local injection B in Figure 1.

[14] More work needs to be done to investigate particle acceleration processes, such as kinetic Alfvén waves and magnetic storage and release, that may accompany or precede the onset of centrifugal interchange [e.g., *Curtis et al.*, 1986] and the compositional mixing that could be produced as flux tubes move inward and outward through the magnetosphere.

[15] **Acknowledgments.** This research was supported by JPL Contract 959930 with SwRI. Helpful comments by Drs. M. F. Thomsen and D. J. McComas are greatly appreciated.

References

Curtis, S. A., et al. (1986), The centrifugal flute instability and the generation of Saturn kilometric radiation, *J. Geophys. Res.*, *91*, 10,989–10,994.
Gurnett, D. A., et al. (2004), The Cassini radio and plasma wave science investigation, *Space Sci. Rev.*, *114*, 395–463.
Hill, T. W. (1976), Interchange stability of a rapidly rotating magnetosphere, *Planet. Space Sci.*, *24*, 1151–1154.
Hill, T. W., et al. (1981), Corotating magnetospheric convection, *J. Geophys. Res.*, *86*, 9020–9028.
Hill, T. W., et al. (2005), Evidence for rotationally driven plasma transport in Saturn's magnetosphere, *Geophys. Res. Lett.*, doi:10.1029/2005GL022620, in press.
Kivelson, M. G., et al. (1997), Intermittent short-duration magnetic field anomalies in the Io torus: Evidence for plasma interchange?, *Geophys. Res. Lett.*, *24*, 2127–2130.
Mauk, B. H., et al. (2005), Energetic particle injections in Saturn's magnetosphere, *Geophys. Res. Lett.*, doi:10.1029/2005GL022485, in press.
Richardson, J. D., and E. C. Sittler Jr. (1990), A plasma density model for Saturn based on Voyager observations, *J. Geophys. Res.*, *95*, 12,019–12,031.
Siscoe, G. L., and D. Summers (1981), Centrifugally driven diffusion of Iogenic plasma, *J. Geophys. Res.*, *86*, 8471–8479.
Thorne, R. M., et al. (1997), Galileo evidence for rapid interchange transport in the Io torus, *Geophys. Res. Lett.*, *24*, 2131–2134.
Yang, Y. S., et al. (1994), Numerical simulation of torus-driven plasma transport in the Jovian magnetosphere, *J. Geophys. Res.*, *99*, 8755–8770.
Young, D. T., et al. (2004), Cassini Plasma Spectrometer investigation, *Space Sci. Rev.*, *114*, 1–112.

N. André, Centre d'Etude Spatiale des Rayonnements, 9 avenue du Colonel Roche, 31028 Toulouse, France. (nicolas.andre@cesr.fr)
J. L. Burch, F. Crary, J. Goldstein, and D. T. Young, Southwest Research Institute, P. O. Drawer 28510, San Antonio, TX 78228-0510, USA. (jburch@swri.edu; fcrary@swri.edu; jgoldstein@swri.edu; dyoung@swri.edu)
A. J. Coates, University College London Mullard Lab, Holmbury St Mary, Dorking, Surrey, RH5 6NT, UK. (ajc@mssl.ucl.ac.uk)
T. W. Hill, Rice University, Department of Physics and Astronomy, MS 108, Houston, TX 77005, USA. (hill@rice.edu)
W. S. Kurth, University of Iowa, Department of Physics and Astronomy, Iowa City, IA 52242, USA. (william-kurth@uiowa.edu)
E. C. Sittler Jr., NASA-GSFC, Greenbelt, MD 20771, USA. (edward.c.sittler@nasa.gov)